Applied Radiation and Isotopes 100 (2015) 27–31

Contents lists available at ScienceDirect

Applied Radiation and Isotopes

journal homepage: www.elsevier.com/locate/apradiso

Evaluation of characteristic-to-total spectrum ratio: Comparison between experimental and a semi-empirical model

A.H. Lopez Gonzales [a], A. Tomal [b], P.R. Costa [a,*]

[a] Laboratory of Radiation Dosimetry and Medical Physics, Physics Institute of São Paulo University, 66318 São Paulo, SP, Brazil
[b] Physics Institute "Gleb Wataghin", Universidade Estadual de Campinas, 13083-859 Campinas, SP, Brazil

HIGHLIGHTS

- Primary X-ray spectra were measured in the range of 80–150 kV.
- Primary X-ray spectra were computed using the TBCmod code, from 80 to 150 kV.
- Characteristic to total spectrum ratio was used to validate the TBCmod code.
- X-ray spectra computed with TBCmod are in good agreement with experimental results.

ARTICLE INFO

Article history:
Received 30 July 2014
Received in revised form
20 December 2014
Accepted 8 January 2015
Available online 9 January 2015

Keywords:
Characteristic-to-total spectrum ratio
X-ray spectrum
CdTe detector.

ABSTRACT

Primary X-ray spectra were measured in the range of 80–150 kV in order to validate a computer program based on a semiempirical model. The ratio between the characteristic and total air Kerma was considered to compare computed results and experimental data. Results show that the experimental spectra have higher first HVL and mean energy than the calculated ones. The ratios between the characteristic and total air Kerma for calculated spectra are in good agreement with experimental results for all filtrations used.

1. Introduction

Since the discovery of the X-ray radiation by Wilhelm Roentgen in 1985, many applications of X-ray beams have been developed. In these developments, special progress can be observed in medical applications for both therapy and diagnosis of diseases. Various issues are important for these medical applications of X-rays. A very important topic is the estimation of radiation doses of patients submitted to therapeutic or diagnostic procedures, which is strongly dependent of the radiation spectra. These spectra are also important for formulating radiation shielding models. On the other hand, routine measurements of X-ray spectra in diagnostic radiology are uncommon due to the complexity of the measurement procedures (Bhat et al., 1998). However, theoretical and semiempirical models have been developed in order to assist the estimation of the spectrum emitted by specific X-ray tube for energies in diagnostic range (Archer and Wagner, 1988; Baird, 1981; Birch and Marshall, 1979; Boone et al., 1997; Boone and Seibert, 1997; Tucker et al., 1991).

A semiempirical model for generating tungsten target X-ray spectra was proposed by Tucker et al. (1991) (TBC model). However, as originally presented, the TBC model fails in situations where it is necessary the production of X-ray spectra to an arbitrary waveform. The original model cannot also provide a realistic calculation of the spectra adopting the air Kerma quantity for the resulting amplitude. The modified TBC model, hereafter called TBCmod (Costa et al., 2007) was used in the present work. This model takes into account the waveform and a representation of the calculated spectra using the air Kerma quantity (Costa et al., 2007). The performance of the proposed model was evaluated by comparing values of mean energy and first half value layer (HVL) from computed and measured spectra for different voltages and filtrations. Finally, to evaluate the contribution of the characteristic photons to total spectrum, the ratio between characteristic-to-total spectrum was calculated (both measured and computed spectra) and compared.

* Corresponding author.
E-mail address: pcosta@if.usp.br (P.R. Costa).

http://dx.doi.org/10.1016/j.apradiso.2015.01.011
0969-8043/

2. Materials and methods

2.1. X-ray spectra measurements and corrections

In the present work, the x-ray spectra were measured by a CdTe detector, model XR-100T-CdTe (Amptek Inc.). This device is an X- and Gamma ray detector mounted on a two-stage thermoelectric cooler. The Cadmium Telluride detector (CdTe) has a nominal area of 9 mm^2 and a thickness of 1 mm with a Schottky diode structure and Peltier cooling. The other element of the spectroscopy system was an Amptek PX4 processor that includes digital pulse shaping amplifier, integrated multichannel analyzer and power supplies.

The model XR-100T-CdTe has a Be window with 100 μm of thickness. Due to its high stopping power, CdTe detector is a good option for detecting photons with energies above 30 keV (Redus et al., 2009). On the other hand, a tungsten collimator with 2 mm diameter and 2 mm thickness and a brass spacer were used.

A Philips MG 450 X-ray system was used for generating the X-ray spectra. It consists of a control unit MGC 30 and a MCN 421 industrial X-ray tube with stationary Tungsten target. A constant-potential generator operating at tube voltage between 40 and 150 kV was used as power supply for the X-ray tube. The measurements were conducted with additional filters of Al with 3.04 mm, 4.71 mm and 5.98 mm of thicknesses. Table 1 presents the X-ray tube specifications used in this work. The X-ray beam area was defined by a collimator that produced a field of 6.91 cm × 5.76 cm diameters at 1 m of the focal spot.

Measurements of the air Kerma were made using an electrometer Unidos E (PTW), coupled to a 30 cm^3 PTW ionization chamber, model TW 23361. The ionization chamber and CdTe detector were located at 5.45 m and 5.60 m of the X-ray tube focal spot, respectively.

The energy calibration, linearity and resolution were determined using ^{241}Am and ^{152}Eu calibration sources. In CdTe detectors, the centroid of the photopeak are shifted by the asymmetry due to hole tailing effect. This centroid shift increases with energy (Redus et al., 2009). To correct this effect, it was used the peak channel rather than the centroid for identify photopeak energies of the ^{241}Am and ^{152}Eu sources, 59.4 keV and 121.7 keV, respectively. Origin 8.5.1 (OriginLab, Co.) software was used to fit the energy distribution for each calibration source, using the Gaussian distribution option of the fitting program.

The detector's response was corrected using a stripping procedure (Castro et al., 1984), considering the detector efficiency, escape peaks of Cd and Te K X-rays and escape of Compton-scattered photons. The response function was determined by Monte Carlo simulation. The simulation of the detector response was based on a previous work (Tomal et al., 2012) for mammographic energy range from 5 to 40 keV, and extended for diagnostic range, from 5 to 160 keV (Tomal et al., in press).

2.2. Software to generate semiempirical X-ray spectra

The TBCmod was published in a previous work (Costa et al., 2007). This code, used to generate diagnostic X-ray spectra, is based on the semiempirical TBC model (Tucker et al., 1991). The

Table 1
X-ray tube specifications.

Tube	Philips MCN 421
Type N°	9421 172 57032
Target	Tungsten
Target angle	22°
Emergent beam angle	30°
Inherent filtration value	2.2 mm Beryllium
Ripple	2.5 kV max.

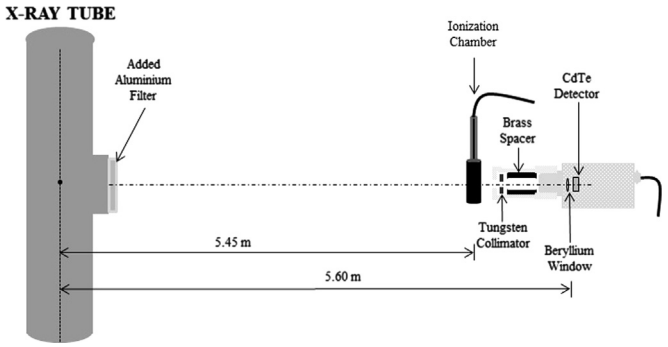

Fig. 1. Experimental setup to measure the spectra. The figure represents the Philips MG 450 X-ray system with the additional filter and the detection system composed by the ionization chamber and the spectroscopy device.

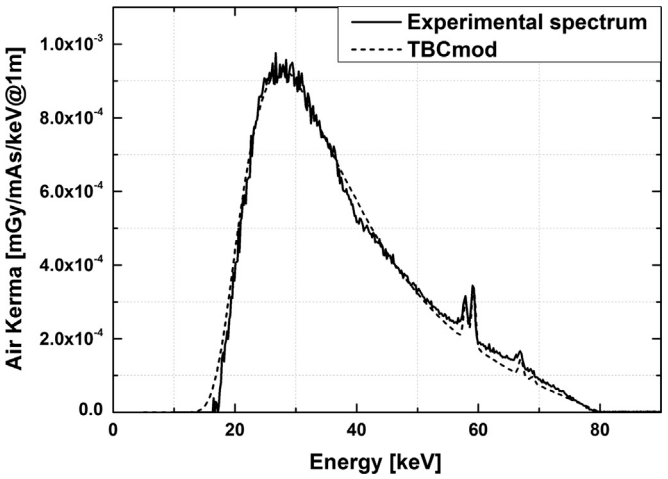

Fig. 2. Comparison between experimental (solid line) and computed (dashed line) data for 80 kV tube potential and 3.04 mm of additional Aluminum filtration.

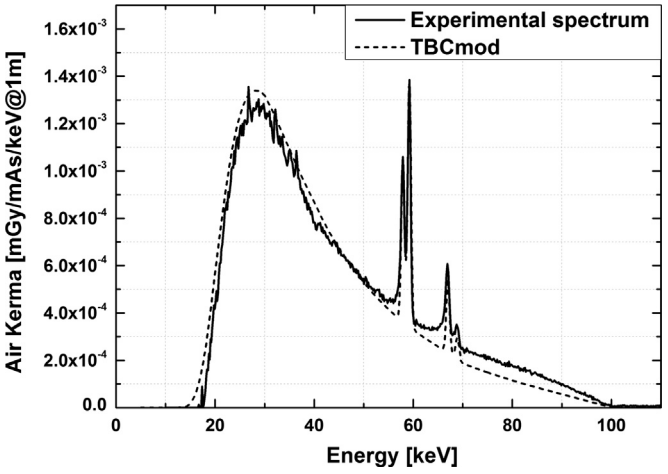

Fig. 3. Comparison between experimental (solid line) and computed (dashed line) data for 100 kV tube potential and 3.04 mm of additional Aluminum filtration.

TBC model introduces a relativistic correction factor which is not applied on the derivation of the Birch and Marshall model (Birch and Marshall, 1979; Bissonnette and Schreiner, 1992) and both bremsstrahlung and characteristic X-ray production are assumed to occur at varying depths within the target (Tucker et al., 1991). In order to take into account the waveform and a representation of the calculated spectra using the air Kerma quantity, TBC model was modified to produce the TBCmod code. In addition, the TBCmod code is able to produce X-ray spectra for different target

Table 2
First Half Value Layer for 3.04, 4.71 and 5.98 mm of additional Aluminum filtration relating to the experimental and computed results obtained using the corresponding X-ray spectra.

Voltage (kV)	Experimental (mmAl)			TBCmod (mmAl)		
	3.04 mmAl	4.71 mmAl	5.98 mmAl	3.04 mmAl	4.71 mmAl	5.98 mmAl
80	3.23	4.04	4.51	2.86	3.69	4.19
90	3.68	4.59	5.12	3.14	4.06	4.62
100	4.14	5.12	5.69	3.41	4.39	4.98
110	4.59	5.63	6.22	3.65	4.68	5.3
120	5.06	6.11	6.72	3.88	4.94	5.59
130	5.49	6.57	7.20	4.10	5.19	5.84
140	5.95	7.02	7.65	4.32	5.41	6.08
150	6.41	7.48	8.09	4.53	5.64	6.30

Table 3
Mean energy for 3.04, 4.71 and 5.98 mm of additional Aluminum filtration relating to the experimental and computed results obtained using the corresponding X-ray spectra.

Voltage (kV)	Experimental (keV)			TBCmod (keV)		
	3.04 mmAl	4.71 mmAl	5.98 mmAl	3.04 mmAl	4.71 mmAl	5.98 mmAl
80	38.9	42.3	44.1	37	40.6	42.5
90	42.2	45.9	47.9	39.2	43.1	45.4
100	45.5	49.3	51.5	41.3	45.4	47.8
110	48.7	52.7	54.9	43.1	47.4	49.9
120	52.0	56.0	58.3	44.9	49.3	51.9
130	55.1	59.1	61.5	46.6	51.1	53.8
140	58.3	62.4	64.7	48.3	52.9	55.6
150	61.6	65.7	68.0	50	54.7	57.5

Table 4
The ratio between the characteristic-to-total X-ray spectrum, R, calculated using the corresponding X-ray spectra.

Voltage (kV)	Experimental			TBCmod		
	3.04 mmAl	4.71 mmAl	5.98 mmAl	3.04 mmAl	4.71 mmAl	5.98 mmAl
80	0.010	0.017	0.017	0.011	0.015	0.018
90	0.030	0.039	0.047	0.027	0.036	0.042
100	0.049	0.058	0.068	0.043	0.056	0.064
110	0.062	0.074	0.084	0.057	0.072	0.081
120	0.073	0.087	0.093	0.068	0.085	0.095
130	0.083	0.094	0.103	0.077	0.095	0.105
140	0.090	0.101	0.109	0.085	0.103	0.113
150	0.095	0.105	0.112	0.091	0.109	0.119

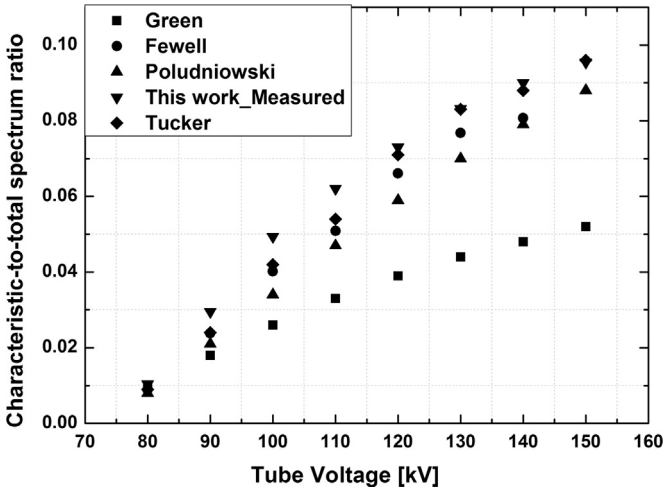

Fig. 4. Comparison between the experimental result at 3.04 mm additional aluminum filtration and literature data (Fewell et al., 1981; Green and Cosslett, 1961, 1968; Poludniowski, 2007; Tucker et al., 1991).

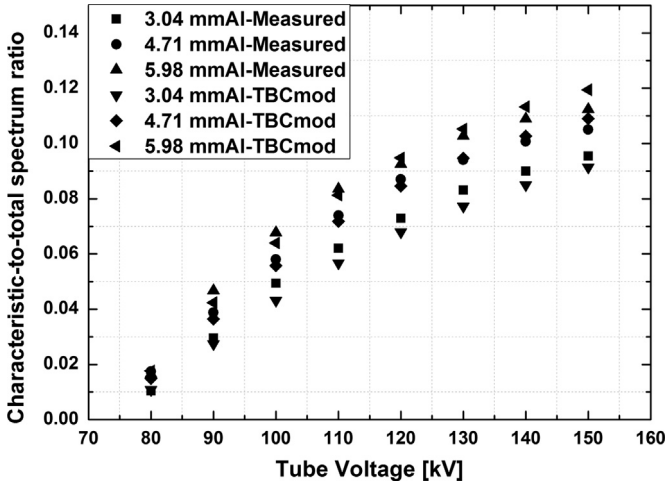

Fig. 5. Ratio of characteristic-to-total spectrum for experimental and computed spectra at 3.04, 4.71 and 5.98 mm of additional aluminum filtration.

angles and a wide range of X-ray tube potentials.

2.3. Characteristic-to-total spectrum ratio

Previous works attempt for the criteria of characteristic-to-total spectrum area for validating the amplitude of the characteristic peaks of the X-ray spectrum (Archer and Wagner, 1988; Ay et al., 2005; Bhat et al., 1998). Characteristic-to-total spectrum ratio, R, was adopted to evaluate the fractional contribution of the characteristic photons in the total spectrum. It is defined as the ratio of areas under each characteristic peak and the total spectrum. Therefore, considering S_C as the area under the characteristic peaks and S_T as the area under the complete spectrum, the characteristic-to-total spectrum ratio can be defined as:

$$R = \frac{S_C}{S_T} \tag{1}$$

In the present work, all S_C and S_T areas of the experimental spectra were calculated using the Origin 8.5.1 (OriginLab, Co.) software. S_T and S_C were determined using Integration and Polygon Area tools, respectively. These procedures use the trapezoidal rule to make such operations.

2.4. First half value layer and mean energy spectra calculation

The computer program used to correct the raw spectrum also compute the first HVL and the mean energy of the spectra from the air Kerma distribution. The first HVL was estimated using an iterative procedure implemented in Matlab 7.14.0 (Mathworks, Inc.) software. The "spline" function of the Matlab software was used to compute the thickness of aluminum that attenuates by half the total air Kerma. The Eq. (2) was used to calculate the mean energy spectra.

$$E_{mean} = \frac{\sum_0^{Emax} EK(E,x)}{\sum_0^{Emax} K(E,x)} \tag{2}$$

In this equation, E is the photon energy and $K(E,x)$ is the air Kerma distribution after the X-ray beam be attenuated by x millimeter of additional aluminum filtration. The number of bins configured on the spectrometer was 1024 (Fig. 1).

3. Results

Three groups of X-ray spectra in the voltage range from 80 to 150 kV were measured to obtain the characteristic-to-total spectrum ratio. The additional filtrations used were 3.04, 4.71 and 5.98 mm of Aluminum. All spectra were measured using the preset-time option of the ADMCA 2.0 acquisition software. The acquisition for all spectra was made at 0.2 mA and 2 min. Three groups of X-ray spectra were computed with the TBCmod code selecting the same parameters used in the measurements. The Fig. 2 shows the comparison between measured and computed spectra at 80 kV using 3.04 mm of additional Aluminum filtration. Fig. 3 presents the comparison at 100 kV and at the same additional filtration. The X-ray spectra show the Tungsten K X-rays lines at 57.9, 59.3, 67.2 and 69.1 keV.

Tables 2 and 3 present the first HVLs and mean energy values for each thickness of additional aluminum filtration and for all evaluated voltage. Table 4 presents R for each thickness of additional aluminum filtration and for all voltage evaluated.

Comparison between measured, computed and data obtained from the literature are presented in the Fig. 4. This figure shows values of the characteristic-to-total spectrum ratio, R, calculated from experimental data measured by Fewell et al. (1981), from theoretical calculation done by Green and Cosslett (1961, 1968), from semiempirical approach evaluated by Tucker et al. (1991), from Monte Carlo calculations done by Poludniowski (2007), and from our experimental data obtained using 3.04 mmAl of additional filter. Fig. 5 shows the ratio of characteristic-to-total spectrum for measured and computed X-ray spectra using different additional filters.

4. Discussion and conclusions

The validation of the TBCmod code was made considering the ratio between the characteristic and total air Kerma for primary x-ray spectra measured in the range of 80–150 kV. Figs. 2 and 3 show that the computed spectra at 80 and 100 kV are in good agreement with the measured spectra. For high energy photons the measured spectrum is slightly higher than the computed spectrum. This difference can be explained by the contribution of photons that penetrate through the collimator material and impinge to the detector. The uncertainties related with each bin in the measured spectra were less than 3%, considering the Poisson distribution of photons per bin. In both cases, the measured spectra are harder than the computed spectra. This is reflected in Tables 2 and 3, since the differences of the first HVLs and mean energies values between measured and computed results, they increases at high tube potentials.

Fig. 4 illustrates that the largest discrepancy in the R value (18% at 110 kV) between experimental results at 3.04 mmAl and published data occur with the Fewell results (Fewell et al., 1981). This discrepancy is attributed to the differences in the anode composition of the two X-ray generator tubes. Fewell had obtained their data from a Computed Tomography X-ray tube with a Tungsten–Rhenium (90/10) alloy target, and our data was obtained using a pure Tungsten target. On the other hand, theoretical results from Green and Cosslett (1961, 1968) are present always lower values then the experimental independent of the applied tube potential, as shown in Fig. 4.

As previously presented, the characteristic-to-total spectrum ratio, R, was considered to validate the TBCmod approach. Fig. 5 demonstrates that the contributions of the characteristic photons to total spectrum are increased with the increasing of the tube potential. The same behavior is present in other published results, independently of its theoretical, experimental, computed or semiempirical origin.

Finally, our results showed that the TBCmod produced X-ray spectra in good agreement with experimental results. The mean difference in R calculated by all studied voltages was 7.2% for 3.04 mmAl of additional filtration. In the same way, the mean differences in R-values for 4.78 mmAl and 5.98 mmAl of additional filtration were 4.6% and 4.9%, respectively.

Acknowledgments

The authors thank FAPESP for financial support under research regular Project 2010/12237-7, CAPES and CNPq/FAPESP funding of Project by INCT-Metrology of Ionizing Radiation in Medicine (Grant no. 573659/2008-7).

References

Archer, B.R., Wagner, L.K., 1988. Determination of diagnostic x-ray spectra with characteristic radiation using attenuation analysis. Med. Phys. 15, 637–641.
Ay, M.R., Sarkar, S., Shahriari, M., Sardari, D., Zaidi, H., 2005. Assessment of different computational models for generation of x-ray spectra in diagnostic radiology

and mammography. Med. Phys. 32, 1660–1675.
Baird, L.C., 1981. X-ray spectra vs attenuation data: a theoretical analysis. Med. Phys. 8, 319–323.
Bhat, M., Pattison, J., Bibbo, G., Caon, M., 1998. Diagnostic x-ray spectra: a comparison of spectra generated by different computational methods with a measured spectrum. Med. Phys. 25, 114–120.
Birch, R., Marshall, M., 1979. Computation of bremsstrahlung X-ray spectra and comparison with spectra measured with a Ge(Li) detector. Phys. Med. Biol. 24, 505.
Bissonnette, J.P., Schreiner, L.J., 1992. A comparison of semiempirical models for generating tungsten target x-ray spectra. Med. Phys. 19, 579–582.
Boone, J.M., Fewell, T.R., Jennings, R.J., 1997. Molybdenum, rhodium, and tungsten anode spectral models using interpolating polynomials with application to mammography. Med. Phys. 24, 1863–1874.
Boone, J.M., Seibert, J.A., 1997. An accurate method for computer-generating tungsten anode x-ray spectra from 30 to 140 kV. Med. Phys. 24, 1661–1670.
Castro, E.D., Pani, R., Pellegrini, R., Bacci, C., 1984. The use of cadmium telluride detectors for the qualitative analysis of diagnostic x-ray spectra. Phys. Med. Biol. 29, 1117.
Costa, P.R., Nersissian, D.Y., Salvador, F.C., Rio, P.B., Caldas, L.V.E., 2007. Generation of calibrated tungsten target x-ray spectra: modified TBC model. Health Phys 92, 24–32.
Fewell, T.R., Shuping, R.E., Hawkins Jr., K.R., 1981. Handbook of Computed Tomography X-Ray Spectra. HHS Publication (FDA), Washington, DC.
Green, M., Cosslett, V.E., 1961. The efficiency of production of characteristic x-radiation in thick targets of a pure element. Proc. Phys. Soc. 78, 1206.
Green, M., Cosslett, V.E., 1968. Measurements of K, L and M shell X-ray production efficiencies. J. Phys. D: Appl. Phys. 1, 425.
Poludniowski, G.G., 2007. Calculation of x-ray spectra emerging from an x-ray tube. Part II. X-ray production and filtration in x-ray targets. Med. Phys. 34, 2175–2186.
Redus, R.H., Pantazis, J.A., Pantazis, T.J., Huber, A.C., Cross, B.J., 2009. Characterization of CdTe detectors for quantitative X-ray spectroscopy. IEEE Trans. Nucl. Sci. 56, 2524–2532.
Tomal, A., Cunha, D.M., Antoniassi, M., Poletti, M.E., 2012. Response functions of Si (Li), SDD and CdTe detectors for mammographic x-ray spectroscopy. Appl. Radiat. Isot. 70, 1355–1359.
Tomal, A., Lopez, A.H., Santos, J.C., Costa, P.R., M.E. Poletti, Monte Carlo simulation of the responce functions of CdTe detectors to be applied in X-ray spectroscopy. Appl. Radiat. Isot. http://dx.doi.org/10.1016/j.apradiso.2015.01.008, in press.
Tucker, D.M., Barnes, G.T., Chakraborty, D.P., 1991. Semiempirical model for generating tungsten target x-ray spectra. Med. Phys. 18, 211–218.